Membrane-Bound Electron Transfer Chain of the Thermohalophilic Bacterium *Rhodothermus marinus*: A Novel Multihemic Cytochrome *bc*, a New Complex III[†]

Manuela M. Pereira, João N. Carita, and Miguel Teixeira*

Instituto de Tecnologia Química e Biológica, Universidade Nova de Lisboa, APT 127, 2780 Oeiras, Portugal

Received July 27, 1998; Revised Manuscript Received November 9, 1998

ABSTRACT: A novel multihemic cytochrome *bc* complex was isolated from the membranes of *Rhodothermus marinus*. It is a complex with a minimum of three subunits (43, 27, and 18 kDa), containing five low-spin heme centers of the B and C types, in a 1:4 ratio. All the C-type hemes are in the same subunit (27 kDa). Three distinct redox transitions, at 235, 80, and −45 mV, were observed by visible redox titrations. The first involves one B- and one C-type hemes, and in the other two transitions one and two C-type hemes are involved, respectively. Spectroscopic data strongly suggest that the two hemes intervening in the last transition are in van der Waals contact, yielding a split Soret band. Electron paramagnetic resonance spectra of the oxidized complex show resonances of five low-spin ferric heme centers. Upon reduction with ascorbate, all these resonances vanish and a new one attributed to the last pair of hemes appears. A $[3Fe\text{-}4S]^{1+/0}$ center copurifies with this complex, having a high reduction potential of +140 mV. No Rieske-type centers are detected in *R. marinus* and no effect is observed in the respiratory rates when the typical bc_1 complex inhibitors are present, suggesting that such a complex is absent in *R. marinus* [Pereira et al. (1994) *FEBS Lett. 352*, 327−330]. The newly isolated cytochrome *bc* complex has quinol:cytochrome *c* or high-potential iron−sulfur protein (HiPIP) oxidoreductase activity, being a functional analogue of the canonical bc_1 complexes; i.e., it is the complex III in *R. marinus*. This complex plays a central role in this bacterium's electron-transfer chain, coupling the electron transfer between the quinols reduced by the dehydrogenases and the HiPIP, the final electron donor to the terminal oxidases [Pereira, M. M., Carita, J. N., and Teixeira, M. (1999) *Biochemistry 38*, 1276−1283].

Rhodothermus marinus belongs to the small number of known thermophilic aerobic bacteria. It is a strict aerobic and moderate halophilic Gram-negative bacterium, with an optimal growth temperature of 65 °C (*1*, *2*). It was classified as a new genus of the heterogeneous group of *Flexibacter*, *Bacteroids*, and *Cytophaga* species (FBC group) (*3*). A preliminary analysis of its membrane-bound electron transport chain suggested some unique properties (*4*), namely, the finding of the first membrane-bound high-potential iron−sulfur protein (HiPIP). Soluble cytochromes have not been detected in *R. marinus*, and the characteristic fingerprint for a Rieske center has not been observed in the membranes by EPR spectroscopy. These findings led us to propose (*4*) that *R. marinus* contains an unusual respiratory chain, in which the HiPIP may substitute for a Rieske-type center or be a direct electron donor for a terminal oxidase. *R. marinus* contains menaquinone 7 as the major quinone (*5*).

Most aerobic microorganisms studied in bioenergetics terms belong to the group of purple bacteria. Due to their phylogenetic relation to mitochondria, these bacteria contain membrane-bound electron-transfer complexes rather similar to the mitochondrial ones—NADH:quinone oxidoreductase (complex I), succinate:quinone oxidoreductase (complex II), and quinol:cytochrome *c* oxidoreductase (complex III). This similarity can also be extended to complex IV, although bacteria can express multiple and diverse terminal oxidases that vary in terms of substrates and metal centers as well as affinity toward oxygen.

The branching of bacterial electron transport chains can also occur at the level of complex III when the electron flow is processed directly to the terminal oxidases that use quinol as substrate. In all bacteria reported to date, the role of complex III, i.e., quinol:cytochrome *c* oxidoreductase, is performed by the bc_1 complex, which contains a dihemic cytochrome *b*, a Rieske protein, and a cytochrome *c* as major and essential subunits for electron transfer (*6*).

Studies on organisms from phylogenetically distant branches revealed in recent years the presence of new families of electron-transfer complexes. The archaeal domain is such an example where unique complexes have been described (*7*−*11*), which appear to consist of supercomplexes containing a bc_1-like subunit and a terminal oxidase. The finding of two terminal oxidases in *R. marinus*, reported in the literature as cytochrome *c* oxidases, demanded the presence of a cytochrome *c* reductase in this bacterium. However, the absence

[†] M.M.P. is the recipient of a grant from the PRAXIS XXI program (BD/2758/94). The work was supported by PRAXIS XXI grants, by European Commission Grant Bio4-CT96-0413, and by European Union G-Project on Biotechnology of Extremophiles (Bio4-CT96-0488).

* Corresponding author: Phone 351-1-4469844; Fax 351-1-4428766; E-mail miguel@itqb.unl.pt.

[1] Abbreviations: TMPD, *N*,*N*,*N*′,*N*′-tetramethyl-*p*-phenylenediamine; TMBZ, 3,3′,5,5′-Tetramethylbenzidine; HiPIP, high-potential iron−sulfur protein; DM, dodecyl β-D-maltoside; EPR, electron paramagnetic resonance; DBMIB, 2,5-dibromo-3-methyl-6-isopropyl-*p*-benzoquinone.

10.1021/bi9818063 CCC: $18.00
Published on Web 01/08/1999

of the characteristic fingerprint for a Rieske center and the inefficiency of the typical inhibitors of bc_1 complex suggested the presence of a different complex III.

In this paper we report the physicochemical properties of an alternative complex III—a novel multihemic cytochrome *bc* complex with menaquinol:HiPIP oxidoreductase activity.

EXPERIMENTAL PROCEDURES

Bacterial Strains and Growth Conditions. In this work a spontaneous nonpigmented mutant of *R. marinus*, strain PRQ-62B, was used. This strain, isolated from the beach Praia da Ribeira Quente at the island of São Miguel, Azores, was shown to be almost identical to the type strain DSM 4253 (*2*). The cells were grown on Degryse medium 162 (*12*), supplemented with 0.25% yeast extract, 0.25% tryptone, and 1% NaCl, at 65 °C and pH 7.5. Reactors of 30 or 300 L were used, at the IBET/ITQB Fermentation Plant, usually with an aeration of 380 L/min and 42 rpm stirring. Different aeration conditions were also tested. Cell density, dissolved oxygen, and pH were continuously monitored. The cells were harvested at the midexponential phase, at the beginning of the stationary phase, or at the late stationary phase, by microfiltration on a Sartocon II system and subsequently centrifuged at 10000*g* and frozen at −70 °C until use.

Membrane Preparation and Solubilization. Frozen cells were thawed and suspended in 20 mM Tris-HCl, pH 8, and then disrupted by passing through a Manton−Gaulin pressure cell at 12 000 psi. Unbroken cells were separated by centrifugation at 10000*g* for 15 min and the suspension obtained was then centrifuged at 200000*g* for 1 h at 4 °C. The membranes were successively washed with 1 mM EDTA in 20 mM Tris-HCl, pH 8, then 1.5 M NaCl in 20 mM Tris-HCl, pH 8, and finally 20 mM Tris-HCl, pH 8. The supernatants as well as the membrane pellets after each step were studied by visible and EPR spectroscopies. The membranes were resuspended in the last buffer with a concentration of approximately 20 mg/mL. The membrane fraction thus obtained was solubilized with dodecyl β-D-maltoside in the proportion of 2 g of detergent/g of protein. This suspension was centrifuged at 200000*g* for 1 h at 4 °C.

Protein Purification. All chromatographic steps were done on Pharmacia HiLoad or LKB HPLC systems, at 4 °C. The detergent-solubilized extract was applied to a fast flow DEAE column, using as buffer 20 mM Tris-HCl, pH 8, and 0.1% DM, and eluted in a linear gradient of 0−50% 1 M NaCl. The heme-containing fraction was then applied to a chelating Sepharose fast flow column saturated with Cu^{2+} and equilibrated with 20mM Tris-HCl, pH 8, and 0.1% DM. The fraction containing the cytochrome *bc* was eluted in a 0−10% 125 mM imidazole linear gradient and then applied to a Q-Sepharose column. This column was eluted in 20 mM Tris-HCl, pH 8, and 0.1% DM with a linear gradient of 0−50% 1 M NaCl. The fraction containing cytochrome *bc* complex was finally purified in a gel-filtration Superose 6 column, eluted with 20 mM Tris-HCl, pH 8, 0.1% DM, and 200 mM NaCl. By this procedure, 75 mg of complex *bc* was obtained from 8 g of total protein in crude membranes.

Heme Determination, Extraction, and HPLC Analysis. Heme content was measured by pyridine hemeochrome, with molar absorptivities of $\epsilon_{r-o,550-535} = 23.97\ mM^{-1}\ cm^{-1}$ for heme C and $\epsilon_{r-o,556-540} = 23.98\ mM^{-1}\ cm^{-1}$ for heme B (*13*). Noncovalently bound hemes were extracted according to ref *14*.

Electrophoresis. The cytochrome *bc* complex is highly hydrophobic, showing a strong tendency to aggregate. Different types of SDS−PAGE (Laemmli system, tricine SDS−PAGE, and gradient acrylamide) and different sample preparation procedures were assayed, namely, to clarify the minimal number of subunits. The best procedure was achieved with a tricine SDS−PAGE as described by Schägger and von Jagow (*15*) with 10% T/2% C in the presence of 0.1% DM in the gel as well as in the running buffer; the samples were incubated overnight with the sample loading buffer containing also 8 M urea. The heme staining procedure followed Goodhew et al. (*16*).

Spectroscopic Techniques. Electronic spectra were obtained on a Beckman DU-70 or on an OLIS DW2 spectrophotometer, at room and liquid nitrogen temperatures. EPR spectra were measured with a Bruker ESP-380 spectrometer equipped with an Oxford Instruments ESR-900 continuous-flow helium cryostat. Parallel-mode EPR was performed with a Bruker dual-mode cavity. EPR spectra obtained under non-saturating conditions were theoretically simulated by the approach of Aasa and Vänngard (*17*). For the analysis of the low-spin heme centers' spectra, several assumptions were made: (i) when only g_{max} is detected, the values generally encountered for g_{med} and g_{min} for this type of heme (e.g., refs *18* and *19*) were used for the simulation; and (ii) when only g_{min} is not observed, it was assumed that $\sum_{i=1}^{3} g_i^2 = 16$ (*20*).

Catalytic Activity Assays. Decylubiquinol:cytochrome *c* oxidoreductase activity was measured by monitoring anaerobically the change in absorbance of horse heart cytochrome *c* at 550 nm at room temperature. Quinols were prereduced with dithiothreitol. All assays were carried out in 20 mM Tris-HCl buffer, pH 8, containing 0.1% DM.

Redox Titrations. Anaerobic potentiometric titrations were followed by visible spectroscopy, at room temperature and pH 7, with the following as redox mediators, each at a final concentration of 2 μM: *N*,*N*-dimethyl-*p*-phenylenediamine, 1,2-naphthoquinone-4-sulfonic acid, 1,2-naphthoquinone, *N*-methyldibenzopyrazine methosulfate, 5-hydroxy-1,4-naphthoquinone, duroquinone, indigo tetrasulfonate, indigo trisulfonate, indigo disulfonate, and 2-hydroxy-1,4-naphthoquinone. Redox titrations were performed for the cytochrome *bc* fractions eluted from the Q-Sepharose and the Superose 6 columns (two independent titrations for each fraction). The redox potentials are quoted in relation to the standard hydrogen electrode.

The titrations were performed in ∼5 mV reduction steps, monitoring the entire visible spectra from 400 to 700 nm (total of ∼100−150 spectra for each titration). The data sets were first analyzed by following the absolute and differential absorptions at the Soret and α-bands, which allowed a preliminary determination of the redox transitions. The data sets were then deconvoluted manually, by use of MATLAB software, by visual inspection of each individual spectrum and by selective subtractions from the total data set of redox spectra. This analysis allowed the determination of the optical spectrum for each heme center. Once all optical components were deconvoluted, the changes in absorbance at the corresponding maxima at the Soret and α-bands as a function of

the solution redox potential were used to determine the reduction potentials of each heme center. Due to the complexity of the system, the data were fitted to single Nernst equations, without taking into consideration homotropic (electron−electron) or heterotropic (electron−proton) interactions. Although this approach is an approximation, particularly for multihemic proteins, it would be completely arbitrary at this stage to introduce more variables. The assignment of each optical species was then confirmed by selective chemical reductions and by a complete reproduction of the full spectra from the sum of the individual components. The relative contributions of each species were deduced both from the relative absorbances at each maximum as well as by the area underneath the α-band obtained by weighting. This last procedure is much more precise, as the transition probabilities are proportional to the spectral area and not to the absorbance values, and avoids the error associated with different line widths.

RESULTS

Biochemical Properties. Our previous studies strongly suggested that no typical bc_1 complex was present in *R. marinus* (*4*). This result has now been confirmed by a careful screening of both intact membranes and solubilized fractions: EPR resonances characteristic of a Rieske center are not detected, a result corroborated by the absence of any effect on the respiratory rates upon addition of typical inhibitors of this complex. Soluble Rieske proteins, as in *Sulfolobus sp.* strain 7 (*21*), are also not observed in *R. marinus*. However, not only are the two terminal oxidases isolated from *R. marinus* analogous to cytochrome oxidases (our unpublished data) but also preliminary experiments showed that all heme centers in *R. marinus* are reduced by quinols, namely, menadiol, which requires the presence of a menadiol oxidizing complex. Hence, this activity was searched for in the heme complexes isolated from *R. marinus*, leading to the identification of a novel *bc* complex.

Visible and EPR spectroscopies were used to monitor all the heme-containing fractions during the purification, leading to the identification of a fraction with characteristic fingerprints in each spectroscopy (see below). It was not possible to further purify this complex, i.e., its spectroscopic and redox properties, heme content, and subunit composition remained constant after the two last chromatographic steps.

The expression of this complex under the different growth conditions, or growth phases, tested is constant, as judged by EPR spectra of the membrane extracts, indicating a central role of this complex in the *R. marinus* respiratory chain. Most important in what concerns its integrity, the visible, EPR, and redox properties of the isolated complex remained constant from the whole membrane extract.

This complex contains C- and B-type hemes, and so it is named cytochrome *bc* complex. Tricine SDS−PAGE of this complex reveals at least the presence of three subunits with apparent molecular masses of 43, 27, and 18 kDa (Figure 1), and TMBZ staining shows the presence of C-type hemes on the 27 kDa subunit. Only these three bands are always detected, independently of the sample or gel preparations; the bands at higher molecular masses are due to aggregation, since its proportion in relation to the other three subunits depended strongly on the preparation of the sample for the gel assay.

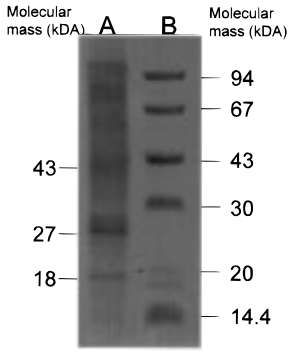

FIGURE 1: (A) Subunit composition of the purified *R. marinus* cytochrome *bc* complex on SDS−PAGE. (B) Molecular mass standards (Pharmacia-Biotech, low molecular weight calibration kit).

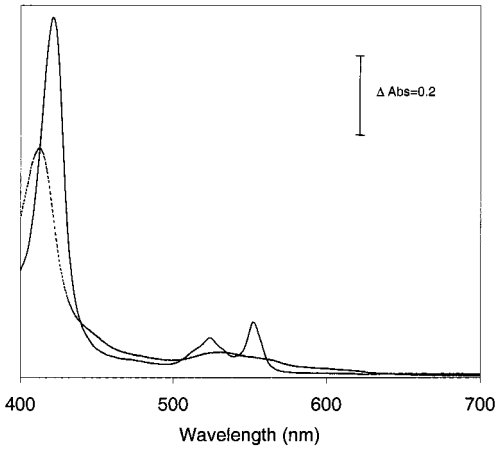

FIGURE 2: Visible spectra of oxidized (- - -) and reduced (—) *R. marinus* cytochrome *bc* complex, at room temperature.

The complex has no TMPD or cytochrome *c* oxidase activity but exhibits quinol:cytochrome *c* oxidoreductase activity. With decylubiquinol and horse heart cytochrome *c* as electron donor and acceptor, respectively, an activity of 22 min^{-1} (mol of cyt *c* /mol of heme) was determined at room temperature. Moreover, the complex is fully reduced by menadiol (see below) and is able to couple menadiol oxidation to HiPIP reduction, directly transferring electrons to HiPIP; the activity is at least 2-fold higher with HiPIP as the electron acceptor (*51*).

The pyridine hemochrome difference spectrum shows α-peaks at 550 and 555 nm, indicating the presence of C- and B-type hemes. However, the relative stoichiometry is rather uncertain, due to the very similar spectral properties of the B- and C-type hemes. On the basis of the visible spectroscopic data, a stoichiometry of 1 heme B: 4 heme C is proposed (see below). Nevertheless, the presence of B-type hemes was unambiguously demonstrated by heme extraction and subsequent HPLC analysis (data not shown).

Visible Spectral Data. The visible spectrum of the oxidized cytochrome *bc* complex is characteristic of low-spin heme centers of the B or C types, with major bands at ∼410 nm (Soret band) and at ∼520 nm (Figure 2A). A very low intensity shoulder at ∼695 nm is present (data not shown), indicating that a methionine is a ligand to at least one of the heme centers. Taking into account the usual molar absorptivities for this band as well as for the α-bands of ferric hemes (*22*), no more than one heme in the complex may have such axial coordination. Features characteristic for high-

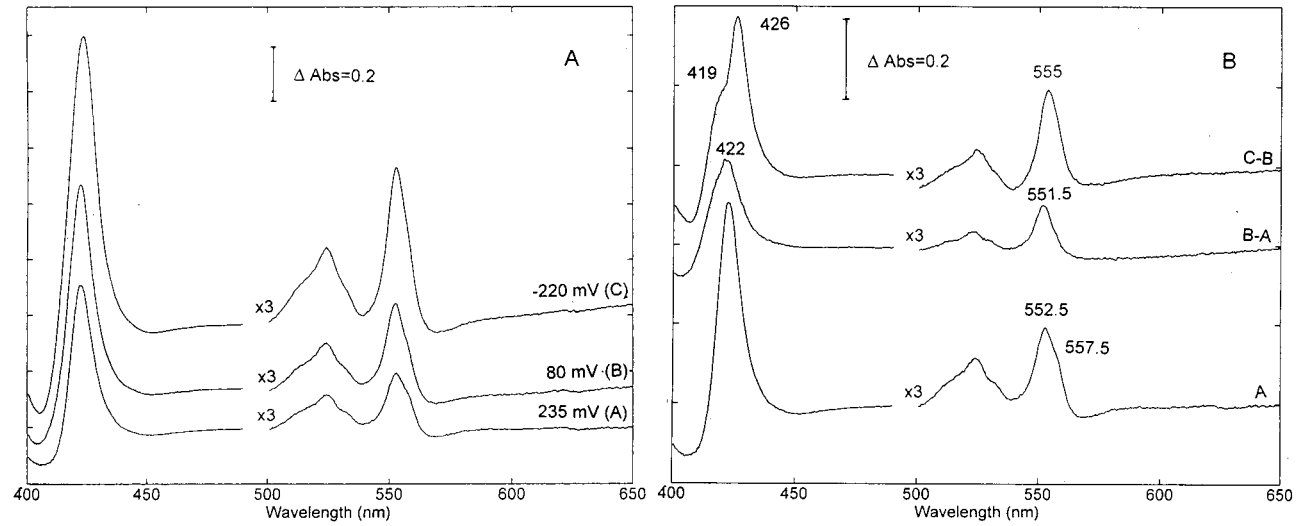

FIGURE 3: Visible redox titration of *R. marinus* cytochrome *bc* complex. (A) Redox spectra at selected redox potentials. (B) Difference spectra at each transition.

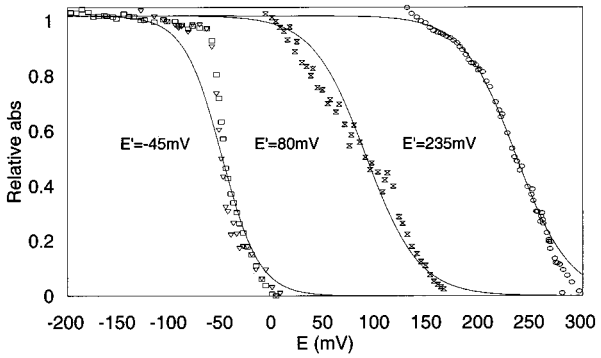

FIGURE 4: Redox titration curves for *R. marinus* cytochrome *bc* complex. The data were obtained at the Soret band maxima; solid lines correspond to Nernst equations with the redox potentials presented in Table 1.

spin heme centers were not observed, corroborating the EPR spectral data (see below) and the absence of reactivity upon incubation of the reduced complex with CO. The same level of reduction is obtained with menadiol or sodium dithionite, indicating that the complex is fully reduced with the quinol. An α-band at 554 nm with a shoulder at 558 nm and a Soret band at 423 nm are observed for the reduced complex (Figure 2B). A complete deconvolution of the reduced spectrum was obtained on the basis of the redox titration data and by selective chemical reductions using sodium ascorbate (next section).

Visible Redox Titration. Redox titrations were performed for the cytochrome *bc* fractions obtained from the two last chromatographic steps. They both yielded identical redox profiles, in terms of midpoint redox potentials and spectroscopic signatures. Moreover, the same redox potentials could be determined from redox titrations of the entire membrane extract (data not shown). The visible redox titration of the cytochrome *bc* complex at pH 7 reveals three redox transitions (Figures3 and 4), with reduction potentials of 235, 80, and −45 mV. The second and third transitions show a shift from $n = 1$ Nernst equations. This shift may be intrinsic to the system, i.e., a result of homotropic or heterotropic interactions, or it may be due to a bad equilibration with the electrode, although several mediator concentrations were tested. Similar shifts have been repeatedly reported in redox titrations of bc_1 complexes (*23*−*25*) and were observed in the titration of the membrane extract (data not shown). As judged by the EPR data (see below), the second redox transition is most probably associated with a protein conformational change.

Table 1: Maxima of Redox Visible Spectra of Each Cytochrome Component and Respective Reduction Potentials for *R. Marinus* Cytochrome *bc* Complex, at pH 7

cytochrome type	Soret (nm)	α (nm)	E' (mV)
c	422.5	552.5	235
b	422.5	557.5	235
c	422	551.5	80
c	426/419[a]	555	−45

[a] Shoulder.

Integration of the α-bands associated with each transition gives a relative intensity of 2:1:2. In the first transition, one cytochrome *c* and one cytochrome *b* are involved (Table 1), since at the end of this transition a redox spectrum with a Soret maximum at 422.5 nm and an α-band peak at 552.5 nm with a shoulder at 557.5 nm is observed (Figure 3A,B, spectrum A). The corresponding spectrum at liquid nitrogen temperature, obtained by substoichiometric reduction of the complex with sodium ascorbate, has a much higher resolution (Figure 5A,B): two α-bands with maxima at 549 and 554 nm are clearly observed. The two hemes have the same reduction potential, within ±10 mV. The second transition yields a redox spectrum characteristic of low-spin cytochrome *c* (Figure 3A,B, spectrum B, and Table 1). One of the hemes with the highest reduction potential may be tentatively assigned to that with the iron ion axially bound to a methionine (*22*, *26*).

The last transition corresponds to an optical species whose assignment is complex. The Soret band has a maximum at 426 nm, with a pronounced shoulder at 419 nm, while the α-band has a maximum at 555 nm (Figure 3A,B, spectrum C). At liquid nitrogen temperature, the α-band is highly asymmetric with a maximum at 549 nm and a broad tail extending to higher wavelength (Figure 5, spectrum C − B); moreover, a hyperchromic shift is observed at that temperature. In contrast to the first transition, two well separated α-bands are not observed. The absorbance changes

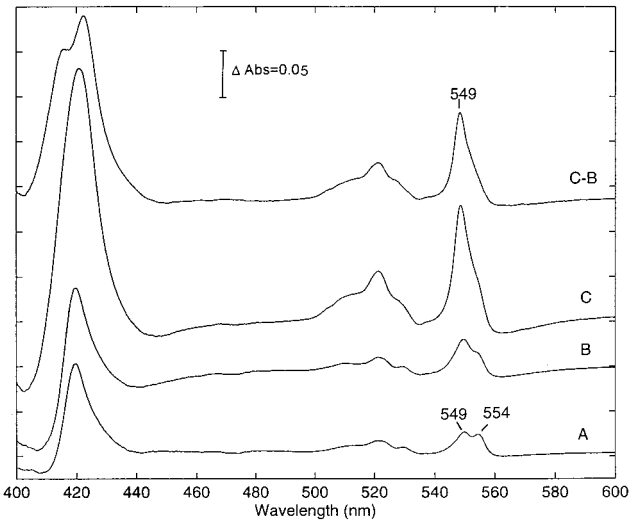

FIGURE 5: Visible spectra of *R. marinus* cytochrome *bc* complex at liquid nitrogen temperature. (A, B) Successive reduction with sodium ascorbate; (C) total reduction with sodium dithionite.

at all the three wavelengths (419, 426, and 555 nm), observed at room temperature, follow exactly the same redox behavior. Since the relative area of the α-band, as well as the intensity of the Soret peak, at room temperature are identical to those of the first optical transition and the double of the second one, this last transition is assigned to two hemes (see below the EPR analysis). Possible artifacts due to the redox mediators may be excluded, as the independent spectra obtained with sodium ascorbate and sodium dithionite as reductants show exactly the same line shapes. Moreover, the same optical species is observed with the entire membrane solubilized extract (data not shown).

EPR Spectroscopy. The EPR spectrum of the as-isolated (oxidized) cytochrome *bc* complex shows several resonances characteristic of low-spin ferric heme centers, with g_{max} from 3.32 to 2.78 (Figure 6, spectrum A). This spectrum is remarkably similar to that of the entire membrane extract (data not shown), showing that indeed this complex is one of the major components of *R. marinus* membranes. A very minor intensity high-spin ferric heme center resonance was detected in some preparations with $g \sim 6$. The low-spin resonances were deconvoluted by theoretical simulation of the spectrum obtained under nonsaturating conditions (Figure 6, Table 2). A total of five low-spin heme centers describes well the overall line shape. However, it is difficult to ascertain an exact stoichiometry, since several assumptions had to be made, as described in the Materials and Methods Section. Moreover, the $g_{max} = 3.32$ and the other two sets of heme resonances have different relaxation properties; a microwave power of 0.24 mW was used for the spectral simulation, a value at which the $g_{max} = 3.02$, 2.80 and 2.78 species are slightly saturated.

Upon reduction with sodium ascorbate or menadiol, all these heme resonances vanish; a new set of resonances with $g_{max} = 2.88$ and $g_{med} = 2.30$ develops (Figure 6, spectrum G), which disappears upon reduction with sodium dithionite or excess menadiol. The intensity of these new resonances in relation to the native spectra was determined both by manual integration and by theoretical simulation of the new species, with the same assumptions as above. By either approach, these new resonances account for two hemes. Since

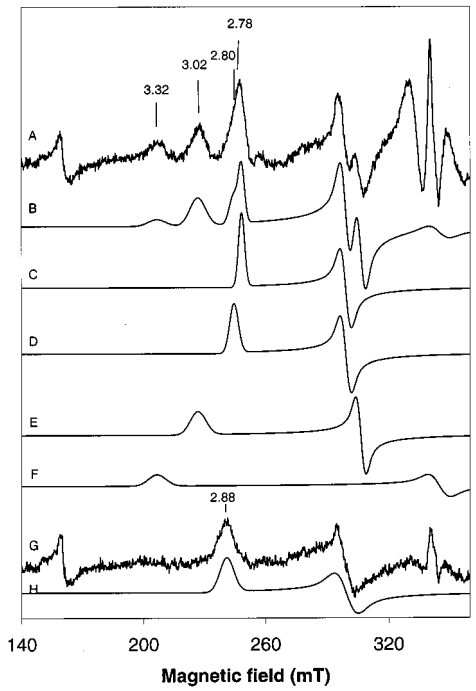

FIGURE 6: (A−F) EPR spectrum of *R. marinus* oxidized cytochrome *bc* complex (A), simulation of the total spectrum (B), and deconvolution of the different components (C−F), using the parameters shown in Table 2. (G, H) EPR spectrum of the cytochrome *bc* complex reduced with ascorbate (G) and respective simulation (H). Microwave frequency 9.64 GHz; microwave power 2.4 mW; modulation amplitude 0.9 mT, temperature 10 K.

Table 2: EPR Components and Respective Stoichiometry for *R. marinus* Cytochrome *bc* Complex

redox state	g_{max}	g_{med}	g_{min}	stoichiometry	simulation[a] (Figure 6)
oxidized	3.32	(2.04)	(1.0)	1	F
	3.02	2.25	(1.3)	2	E
	2.80	2.30	(1.50)	1	D
	2.78	2.30	(1.55)	1	C
partially reduced	2.88	2.30	(1.72)	2[b]	H

[a] Values in parentheses were used for the simulations. [b] In relation to the oxidized spectrum.

these resonances vanish upon reduction with sodium dithionite or excess menadiol, they are assigned to the two heme centers associated with the third redox transition detected in the visible redox titration. The same behavior was obtained with the membrane extract (data not shown).

In the EPR spectrum of the oxidized complex, another strong resonance is observed at $g = 2.027$, 1.940, and 1.830 (Figure 7), which is optimally detected at 4.6 K and starts broadening at ~10 K. With the above-discussed limitations, this resonance integrates to ~0.5 spin per five low-spin heme centers. Hence, at present, it is not possible to decide if this center is in fact a component of the whole complex or if it represents a copurified contaminant, although it is always present in the same proportion in several preparations studied and has not been detected isolated. This center is also reduced in the presence of menadiol, yielding an EPR spectrum at parallel mode, characteristic of an $S = 2$ ground state (data not shown). The magnetic properties of both the oxidized and reduced forms are characteristic of $[3Fe\text{-}4S]^{1+/0}$ centers (*27*). The midpoint redox potential was determined to be 140

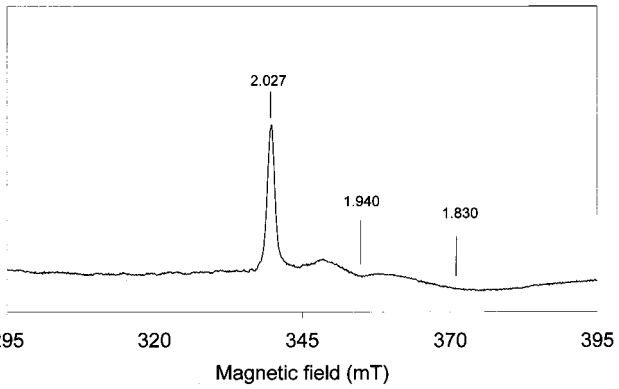

FIGURE 7: EPR spectrum of the oxidized [3Fe-4S] center copurified with the complex, at 4.5 K. Other experimental conditions were as in Figure 6.

mV by an EPR redox titration, performed in both the reductive and oxidative directions (data not shown).

DISCUSSION

Besides complexes I and II analogues (*51*), two distinct terminal oxidases of the caa_3 and cbb_3 types and a cytochrome *c* (our own unpublished data), a novel cytochrome *bc* complex is expressed in the *R. marinus*. This cytochrome is proposed to be complex III of *R. marinus* respiratory chain, appearing as a novel type of electron-transfer component with a rather unique heme organization. The same level of expression of this cytochrome under different growth conditions, or growth phases, indicates a central role of this complex in the *R. marinus* respiratory chain.

The cytochrome *bc* complex contains five low-spin heme centers, of the B and C types, with all the C-type hemes in the same single subunit. While the three heme centers with higher redox midpoint potentials have well-defined optical spectra, the third optical species observed in the visible spectra of cytochrome *bc* is more complex to analyze. Essentially two interpretations can be proposed. The first and most straightforward is to tentatively assign the Soret "shoulder" at 419 nm and the maximum at 426 nm to two distinct heme centers. These two cytochromes would have exactly the same individual redox midpoint potentials and α-bands but quite different Soret bands, in terms of maxima and line shape. A second alternative interpretation is to assign the shoulder at the Soret optical band to a strong electronic interaction between the heme centers, which would yield the split of this band. Due to the low transition probability of the α-band, no splitting in this region is observed at room temperature, but at liquid nitrogen temperature this band is highly asymmetric. This splitting effect is widely observed in chromophore dimers, a particular example being chlorophyll dimers (*28*). Such an interaction occurs when the distance between the chromophores is short and the transition dipole moments are aligned within a certain angle range. In heme proteins it was first described in polymers of horse heart undecapeptide (*29*) and is particularly well depicted in the *Desulfovibrio desulfuricans* (ATCC 27774) dimeric *split Soret* cytochrome (*30*, *31*; our own unpublished data). In this cytochrome the two hemes within each monomer are in van der Waals contact, having an interiron distance of 9 Å (*32*). The redox spectrum of the fully reduced cytochrome is almost identical to that of the last optical transition of the *R. marinus* cytochrome *bc* complex. In such a situation, hyper- or hypochromic shifts may occur. While for the *split Soret* cytochrome these effects seem to be absent (possibly due to the very peculiar geometric arrangement of the four hemes in the dimer (*32*)), for the *R. marinus* cytochrome a hyperchromic effect is detected at liquid nitrogen temperature. Hence, the quantification of two hemes for the last transition relies mainly on the EPR data. The apparent split at the Soret and α-bands and the hyperchromic effect, as well as the fact that the two heme centers have the same *g*-values and redox behaviors, which strongly points to the same heme structure (i.e., either of the C or B type), lead us to prefer the hypothesis that the third transition involves a heme−heme electronic interaction.

In the EPR spectrum of cytochrome *bc* complex there is no evidence for a magnetic heme−heme interaction. However, such interaction is also not observed in the EPR spectra of *D. desulfuricans split Soret* cytochrome (*31*) and of other multihemic cytochromes (e.g., refs *33*−*35*). A detailed theoretical study of dipolar interactions in multihemic cytochromes has shown that the dipolar interaction vanishes at certain relative orientations of the g-tensor of the paramagnetic heme centers (*36*). It remains to be explained why the resonances with $g_{max} = 2.88$ are not observed either in the oxidized membrane extract or in the oxidized cytochrome *bc*. At present, it can only be speculated that a redox-linked conformational change occurs. Similar behavior has been observed in multihemic proteins, such as the hexaheme cytochromes from *Desulforomonas acetoxidans* (*35*), *Nitrosomonas europea* hydroxylamine oxidoreductase (*37*), and tetrahemic cytochromes c_3 from *Desulfovibrio* species (e.g., refs *20* and *38*). Unfortunately, no three-dimensional structures are available for these proteins in different oxidation states.

As the *R. marinus* cytochrome *bc* complex exhibits quinol:cytochrome *c* oxidoreductase activity, it is a functional analogue of the typical bc_1 complexes, which were thought either to be absent or to have distinct characteristics in this organism (*4*, *39*). The *R. marinus* cytochrome *bc* complex reduces the HiPIP (see ref *51*) acting as a menaquinol:HiPIP oxidoreductase. This type of activity had already been indirectly suggested in the case of photosynthetic electron transport chains where HiPIP could be substituting for cytochrome c_2 transferring electrons between the bc_1 complex and the bacterial reaction center (*40*). To our knowledge, *R. marinus* cytochrome *bc* bears no similarities with any heme complex so far described. This complex is unique in terms of heme composition and also it most probably contains a pair of hemes in close contact. Its difference from the bc_1 complex is also reflected in the absence of any effect of the typical inhibitors of this complex, such as antimycin A, mixothyazol, and DBMIB.

The heme centers in *R. marinus* cytochrome *bc* complex cover a wide redox potential range, from −45 to +235 mV, at pH 7. Having the lower reduction potentials, the pair of hemes in contact may represent the electron entry site from the quinols. The functional implications of this geometric arrangement remains to be determined, but a strong redox interaction between the two redox centers is certainly operative. Although in simple electrostatic terms an anticooperative effect would be expected, positive redox cooperativity has been shown to occur in multihemic cytochromes, linked to protonation and conformational changes (*41*). Very interest-

ingly, a recently published three-dimensional structure of mitochondrial bc_1 complexes (*42*) shows that a large conformational change occurs during the electron-transfer process, a fact that could explain the major change observed in the EPR spectrum of the *R. marinus* cytochrome *bc* complex.

The EPR *g*-values for each heme center show a wide spread of ligand fields at the heme iron; however, the *g*-values have proven rather ambiguous in unequivocally identifying the heme iron axial ligands (*43*−*45*). The heme center with $g_{max} = 3.32$ has a quasi-axial ligand field, which in the case of a bishistidinyl coordination would result from a coplanarity of the histidine imidazoles (e.g., ref *46*). All the other heme centers have a rhombic ligand field and the low *g*-values of ∼2.8 suggest a partial deprotonation of the axial histidine(s) for the corresponding heme centers, eventually through a hydrogen bond involving the Nδ_1 of the imidazole ligand (*47*, *48*). The possible role of the [3Fe-4S]$^{1+/0}$ center remains to be determined, as well as whether it is an integral component of the complex.

With the exception of the typical bc_1 complex, no other heme complex with quinol:cytochrome *c* oxidoreductase activity has been reported to date in aerobic microorganisms. A cytochrome *bc* complex from *Natrobacterium pharaonis* was partially characterized (*9*). However, no enzymatic activity has been reported for this complex and both its subunit composition and heme content are very different from those of the *R. marinus* cytochrome *bc* complex. Apart from these complexes, and the tetrahemic subunit of the photosynthetic reaction center (*49*), multihemic proteins have been found mainly in anaerobic bacteria (for a recent review, see ref *22*]. Although in almost all cases the actual physiological function of such proteins is not known, it is nevertheless clear that a rather sophisticated electron-transfer network is operative in these multihemic proteins, enabling an efficient and controlled transfer of electrons within the protein and to or from their physiological partners (e.g., refs *41* and *50*).

In conclusion, the present data provide the characterization of a quinol:cytochrome (HiPIP) oxidoreductase, which couples menadiol oxidation to oxygen reduction, via HiPIP and the terminal oxidases (*51*), being most probably complex III in the *R. marinus* respiratory chain.

ACKNOWLEDGMENT

We thank the IBET fermentation plant for the bacterial growth. *R. marinus* strains were a kind gift from Professor M. da Costa. We are grateful to Professor António Xavier and Robert Anglin for the critical reading of the manuscript.

REFERENCES

1. Alfredsson, G. A., Kristjansson, J. K., Hjörleifsdottir, S., and Stetter, K. (1988) *J. Gen. Microbiol. 134*, 299−306.
2. Nunes, O. C., Donato, M. M., and da Costa, M. S. (1992) *System. Appl. Microbiol. 15*, 92−97.
3. Andrésson, O. S., and Fridjónsson, O. H. (1994) *J. Bacteriol. 176*, 6165−6169.
4. Pereira, M. M., Antunes, A. M., Nunes, O. C., Costa, M. S., and Teixeira, M. (1994) *FEBS Lett. 352*, 327−330.
5. Tindall, B. J. (1991) *FEMS Microbiol. Lett. 80*, 65−68.
6. Trumpower, B. (1990) *Microbiol. Rev. 54*, 101−129.
7. Schäfer, G. (1996) *Biochim. Biophys. Acta 1277*, 163−200.
8. Lübben, M., Arnaud, S., Castresana, J., Warne, A., Albracht, S. P. J., and Saraste, M. (1994) *Eur. J. Biochem. 224*, 151−159.
9. Scharf, B., Wittenberg, R., and Engerlhard, M. (1997) *Biochemistry 36*, 4471−4479.
10. Iwasaki, T., Matsuura, K., and Oshima, T. (1995) *J. Biol. Chem. 270*, 30893−30901.
11. Gleissner, M., Kaiser, U., Antonopoulos, E., and Schäfer, G. (1997) *J. Biol. Chem. 272*, 8417−8426.
12. Degryse, G., Glansdorff, N., and Piérard, A. (1978) *Arch. Microbiol. 117*, 189−196.
13. Berry, E. A., and Trumpower, B. L. (1987) *Anal. Biochem. 161*, 1−15.
14. Lübben, M., and Morand, K. (1994) *J. Biol. Chem. 269*, 21473−21479.
15. Schägger, H., and von Jagow, G. (1987) *Anal. Biochem. 166*, 368−379.
16. Goodhew, C. F., Brown, K. R., and Pettigrew, G. W. (1986) *Biochim. Biophys. Acta 852*, 288−294.
17. Aasa, R., and Vänngard, V. T. (1975) *J. Magn. Reson. 19*, 308−315.
18. Iwasaki, T., Isogai, Y., Iizuka, T., and Oshima, T. (1995) *J. Bacteriol. 177*, 2576−2582.
19. Thomson, A. J., and Gadsby, P. M. A. (1990) *J. Chem. Soc., Dalton Trans.* 1921−1928.
20. Campos, A. P. (1994) Ph.D. Dissertation, Universidade Nova de Lisboa, Portugal.
21. Taylor, C. P. S. (1977) *Biochim. Biophys. Acta 491*, 137−149.
22. Pereira, I. A. C., Teixeira, M., and Xavier, A. V. (1997) *Struct. Bonding 91*, 135−159.
23. Dutton, P. L., Wilson, D. F., and Lee, C.-P. (1970) *Biochemistry 9*, 5077−5082.
24. Rich, P. R., Jeal, A. E., Madgwick, S. A., and Moddy, A. J. (1990) *Biochim. Biophys. Acta 1018*, 29−40.
25. Howell, N., and Robertson, D. E. (1993) *Biochemistry 32*, 11162−11172.
26. Pettigrew, G. W., and Moore, G. R. (1987) *Cytochromes c, Biological Aspects*, Springer-Verlag, Berlin.
27. Hagen, W. R., Dunham, W. R., Johnson, M. K., and Fee, J. A. (1985) *Biochim. Biophys. Acta 828*, 369−374.
28. Sauer, K., Smith, J. R. L., and Schultz, A. J. (1966) *J. Am. Chem. Soc. 88*, 2681.
29. Urry, D. W. (1967) *J. Biol. Chem. 242*, 4441−4448.
30. Liu, M.-C., Costa, C., Coutinho, I. B., Moura, J. J. G., Moura, I., Xavier, A. V., and LeGall, J. (1988) *J. Bacteriol. 170*, 5545−5551.
31. Costa, C. (1994) Ph.D. Dissertation, Universidade Nova de Lisboa, Portugal.
32. Matias, P. M., Morais, J., Coelho, A. V., Meijers, R., Gonzalez, A., Tompson, A. W., Sieker, L., LeGall, J., and Carrondo, M. A. (1997) *J. Biol. Inorg. Chem. 2*, 507−514.
33. Chen, L., Pereira, M. M., Teixeira, M., Xavier, A. V., and LeGall, J. (1994) *FEBS Lett. 347*, 295−299.
34. Pereira, I. A. C., LeGall, J., Xavier, A. V., and Teixeira, M. (1997) *J. Biol. Inorg. Chem. 2*, 23−31.
35. Pereira, I. A. C., Pacheco, I., Liu, M.-Y., LeGall, J., Xavier, A. V., and Teixeira, M. (1997) *Eur. J. Biochem. 248*, 323−328.
36. More, C., Camensuli, P., Dole, F., Guigliarelli, B., Asso, A., Fournel, A., and Bertrand, P. (1996) *J. Biol. Inorg. Chem. 1*, 152−161.
37. Lipscomb, J. D., and Hooper, A. B. (1982) *Biochemistry 21*, 3965−3972.
38. Guigliarelli, B., Bertrand, P., More, C., Haser, R., and Gayda, J. P. (1990) *J. Mol. Biol. 216*, 161−166.
39. Pereira, M. M., Teixeira. M., and Saraste, M. (1996) *Biochim. Biophys. Acta EBEC short Rep. 9*, 222.
40. Bartsch, R. (1991) *Biochim. Biophys. Acta 1058*, 28−30.
41. Louro, R. O., Catarino, T., Salgueiro, C. A., LeGall, J., and Xavier, A. V. (1996) *J. Biol. Inorg. Chem. 1*, 34−38.
42. Zhang, Z., Huang, L., Shulmeister, V. M., Chi, Y.-I., Kim, K. K., Hung, L.-W., Crofts, A. R., Berry, E. A., and Kim, S.-H. (1998) *Nature 392*, 677−684.
43. Teixeira, M., Campos, A. P., Aguiar, A. P., Costa, H. S., Santos, H., Turner, D. L., and Xavier, A. V. (1993) *FEBS Lett. 317*, 233−236.

44. Campos, A. P., Aguiar, A. P., Hervás, M., Ortega, J. M., Regala, M., Navarro, J., Xavier, A. V., deLa Rosa, M., and Teixeira, M. (1993) *Eur. J. Biochem. 216*, 329−341.
45. Medina, M., Louro, R. O., Peleato, M. L., Mendes, J., Gómez-Moreno, C., Xavier, A. V., and Teixeira, M. (1997) *J. Biol. Inorg. Chem. 2*, 225−234.
46. Simpkin, D., Palmer, G., Devlin, F. J., McKenna, M. C., Jensen, G. M., and Stephens, P. J. (1989) *Biochemistry 28*, 8033−8039.
47. Moore, G. R., Williams, R. J. P., Peterson, J., Thomson, A. J., and Mathews, F. S. (1985) *Biochim. Biophys. Acta 829*, 83−96.
48. Quinn, R., Nappa, M., and Valentine, J. S. (1982) *J. Am. Chem. Soc. 104*, 2588−2595.
49. Nitschke, W., and Dracheva, S. (1995) *in Anoxygenic Photosynthetic Bacteria* (Blankenship, E. E., Madigan, M. T., and Bauer, C. E., Eds.) Chapter 36, pp 775−805, Kluwer Academic Publishers, Dordrecht, The Netherlands.
50. Louro, R. O., Catarino, T., LeGall, J., and Xavier, A. V. (1997) *J. Biol. Inorg. Chem. 2*, 488−491.
51. Pereira, M. M., Carita, J. N., and Teixeira, M. (1999) *Biochemistry 38*, 1276−1283.

BI9818063